AN EFFICIENT HIGH-CURRENT MICROTRON

S. P. KAPITZA, V. P. BYKOV, and V. N. MELEKHIN

Physics Laboratory, Institute for Physics Problems, Academy of Sciences, U.S.S.R.

Submitted to JETP editor March 28, 1961

J. Exptl. Theoret. Phys. (U.S.S.R.) **41**, 368-384 (August, 1961)

The construction of a high-current microtron is described, in which electrons are accelerated to 6 — 13 Mev, the pulse currents being 20 — 5 ma. The operation of an efficient lanthanum boride thermionic cathode in the rf field of the accelerating resonator is studied. The efficiency of the accelerator is estimated, and its principal calculated and experimentally confirmed parameters are presented.

1. INTRODUCTION

THE electron cyclotron, which is a cyclic accelerator of relativistic particles in a constant magnetic field and at constant frequency of the accelerating voltage, was first suggested by Veksler.[1] The earliest electron accelerators constructed on the new principle[2-4] were inefficient, and interest in microtrons, as these electron accelerators were subsequently called, disappeared during the rapid development of linear electron accelerators.

The low efficiency of earlier microtrons[2-6,15] resulted from the unsatisfactory conditions of electron injection. The uncontrollability of field emission in the strong field of toroidal resonant cavities and the impossibility of predicting electron trajectories precisely resulted in a low efficiency of capture and of the accelerator as a whole.

Theoretical investigations of phase stability in microtrons[7-9] have shown that the range of phase oscillations is small (0 — 32°). This fact directed our attention to the microtron as an accelerator that can produce beams of bunched electrons with constant energy. On the other hand, the small region of stable motion is the basis for all difficulties regarding particle capture into accelerating orbits. Increased efficiency could therefore not be expected without an essential change in the conditions of injection.

We have proposed[10] a resonator based on electron injection from a thermionic cathode through the direct action of the rf resonator field. The use of a simple cavity shape in the E_{010} mode permitted precise calculations of electron motion in a field of known configuration. The accelerator constructed by us yielded a (pulse) current of 20 ma at 7 Mev, and 5 ma at 13 Mev. The new technique of electron injection into the accelerating mode permitted doubling of the magnet field strength, thus doubling the beam energy without changing the diameters of the orbits. The variation of magnetic field strength also permitted the continuous variation of beam energy, which was thus no longer limited to integral multiples of the rest energy as in previous modes of operation.

It should be noted that several authors have suggested independently that a complicated arrangement of electron trajectories in the resonator could be employed. Thus, Aitken[11] suggested placing the electron emitter within the rf field. Poulin[12] suggested a method of injection in a toroidal resonator which in principle also permitted strengthening of the magnetic field, but motion in the given field could not be calculated simply. No experimental results with resonators of these types have been published.

The present paper describes the construction of a high-current microton and discusses the basic physical principles of this type of accelerator.

2. ACCELERATOR MAGNET AND CHAMBER

The electromagnet and vacuum chamber are shown in Fig. 1. The diameter of the vacuum chamber 1 is 700 mm; its top and bottom are formed by the magnet poles 2, which are separated by 110 mm. The magnet coils 3 wound with 25 × 1 mm copper strip insulated by paper tape are mounted directly on the poles. The coils are cooled by water circulating in rubber tubes 4 that are in contact with the coils.

The upper plate of the magnet is clamped to the pillars 5 in the magnetic circuit by four screws, which at the same time fasten down the rubber gasket 6 between the poles and the chamber wall. This magnet is distinguished by 8-mm compensat-

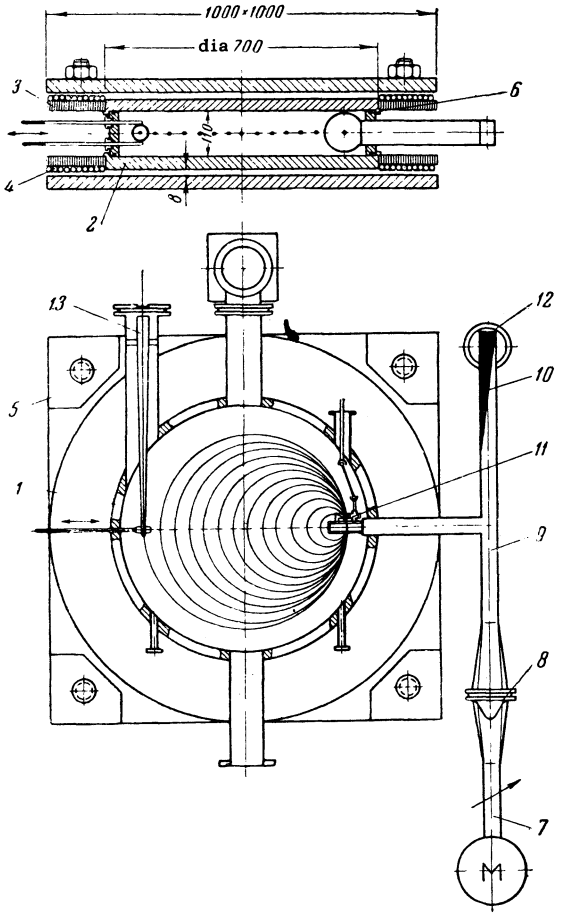

FIG. 1. Microtron vacuum chamber and electromagnet.

ing gaps between the plates and poles. These gaps in the magnetic circuit increase the anisotropy of the demagnetization coefficient of the poles and thus enhance the magnetic field homogeneity in the working space. The effect of the gaps is based essentially on the fact that, with continuity of the tangential field component, the lines of force turn through a greater angle in the air gap than in the iron of the poles. The introduction of these gaps is justified only when the iron of the magnetic circuit and poles is unsaturated. Conventional 12 × 4 mm shims are located at the edges of the poles in order to enlarge the homogeneous field region. The relative field homogeneity depends on the field strength and comprises a few tenths of one percent when the diameter of the working region is about 55 cm in fields up to 1500 oe.

The total weight of the magnet is 1.5 tons; No. 3 steel was used in its construction. The field strength in the chamber reached 2000 oe at 4 kw and 3 amp/mm^2 current density. Power was fed to the magnet from a three-phase selenium rectifier and a motor-generator converter stabilized within 0.1% at 427 cps. The same converter also fed the modulator.

The accelerator chamber and waveguide were evacuated by diffusion pumps with liquid nitrogen traps, to which nitrogen was supplied automatically.[13]

Access to the chamber was obtained by lifting the upper plate together with the pole and coil. After the chamber was closed, hot pumps produced the 10^{-5} mm Hg working vacuum within 15 — 20 min. The numerous insertions and shifts within the chamber were made through rubber and teflon seals in the wall.

The control chamber was separated from the accelerator by a 2-meter shield. The remote electric control was performed with selsyns.

A probe was moved across the chamber to measure the current distribution in the different orbits. The current in the target was registered either oscillographically or by an automatic potentiometer in which the tape motion was synchronized with the probe motion. Figure 4 shows a record obtained in this manner. The target was a water-cooled copper rod or plate coated with a phosphor.

The image of the beam on the target was viewed with a commercial PTU-4 television receiver. Sevenfold magnification of the television screen image permitted the detailed study of the position and size of the beam in any orbit.

3. RADIO-FREQUENCY SYSTEM AND RESONATOR

The rf field in the resonator was excited by means of a standard untunable magnetron and a modulator with a long pulse-shaping line. The rf pulse duration was 3 μsec and its repetition frequency was 427 cps. The waveguide transmission line (Fig. 1) consisted of a phase shifter 7, vacuum port 8, tee 9, water load 10, and resonator 11. Supplementary evacuation of the waveguide can be performed by an oil diffusion pump 12, although evacuation through the resonator produces a sufficiently low pressure. The cooling water circulates first through the load, then through the resonator. Thus the thermocouples measuring the water temperature differential between the input and output of the load and resonator permitted a direct comparison of the power fed to both the load and the resonator. This ratio was usually a little larger than unity.

The most crucial part of the accelerator is the resonator. The first runs were performed with conventional toroidal resonators and 8 — 10 mm accelerating gaps. Very careful selection of the shape and surface of the accelerating gap with direct emission from the copper walls enabled us to attain currents up to 7 ma (with 6 Mev energy in the 12th orbit), but only when the accelerator was tuned very critically.

In our search for an improved injection method and emission control we switched to a cylindrical resonator in which E_{010} oscillations were excited (a "flat" resonator). Electrons in this resonator start from a hot cathode k installed on the flat wall of the resonator (Fig. 2). Inside of the resonator two types of trajectories are possible, the first of which (Fig. 2a) starts at a cathode positioned relatively far from the resonator axis. In this case an electron leaves the resonator when its total energy U is 2 — 2.5 times its rest energy $U_0 = mc^2$; with each successive transit the electron energy is increased by 1 — 1.25 U_0, i.e., 500 — 600 kev. This occurs when the magnetic field is 1 — 1.25 H_0, where $H_0 = 2\pi U_0/\lambda e = 1070$ oe is the magnetic field calculated for the wavelength $\lambda = 10$ cm.

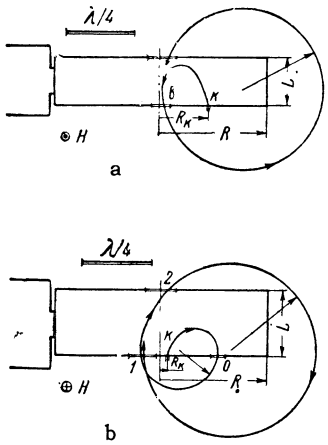

FIG. 2. Electron motion in the resonator.

For trajectories of the second type (Fig. 2b) the cathode is close to the resonator axis. An electron first passes through an additional port O before entering into its resonant orbit, where with each transit its energy is increased by 1.8 — 2.2 U_0 in a magnetic field of 1.8 — 2.2 H_0.

All parameters of electron motion in microtron accelerating modes were calculated. A simulating machine, Prudkovskii's trajectory plotter,[14] was used for preliminary calculations. This machine plots electron paths in a variable electromagnetic field, using a computer for mechanical integration and simulation of the equations of motion.

For a detailed study of electron motion the equations of motion were integrated numerically on the fast Strela computer. The numerical results supplied complete information regarding particle dynamics in the accelerator. Details of the calculation are given in the Appendix.

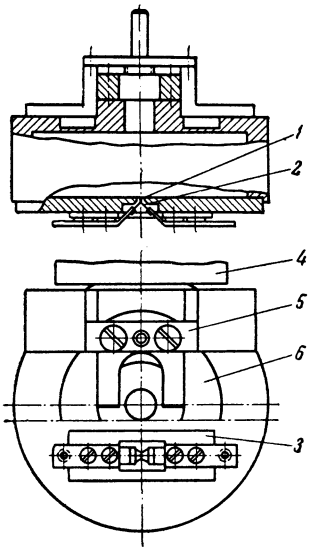

FIG. 3. Cross section of first type of resonator.

Figure 3 is a sketch of the dismountable resonator, made of oxygen-free copper, used for the first mode of electron acceleration. The resonator is excited through a port in its cylindrical wall, which forms a junction with the end of a rectangular waveguide 4. The size of the junction aperture was determined empirically. The Q of the cold resonator when loaded with the waveguide was usually about one-half or one-third of its intrinsic Q.

A simple screw mechanism 5 was used to tune the resonator by bending one of its walls into which a diaphragm 6 (0.2 — 0.3 mm thick) had been inserted. The resonator and its parts around the membrane were water-cooled; the cooling tubes had been soldered to the resonator housing with silver in vacuo.

Table I gives the resonator dimensions R and L, the cathode position (the distance R_k), the constant magnetic field strength H, the amplitude E of the rf electric field, and other data pertaining to the wavelength $\lambda = 10.0$ cm, which are analyzed in Sec. 4.

Table I

Mode	R, cm	L, cm	R_k, cm	H/H_0	H, oe	E, kv/cm	Resonant phase φ_0	Initial phase region $\Delta\varphi$
1	3.83	1.67	1.75	1.1	1180	380	0	0.07
2	3.83	2.31	0.32	1.81	1940	460	0	0.25

4. THE CATHODE AND ELECTRON CAPTURE INTO ACCELERATING MODES

The initial experiments with a flat resonator and tungsten cathode did not produce the required emission and current density. The best cathode, satisfying all requirements, was a lanthanum boride (LaB_6) thermionic cathode (Fig. 3). This cathode 1, a 1.5 mm cube, was cut electrically from a baked rod of the boride. The cube was soldered to a tantalum heater 2, which was 0.2 mm thick and 2 — 2.5 mm wide; the soldering was performed in vacuo at 2000° C with molybdenum disilicide ($MoSi_2$). At 1500 — 1600° C with rf fields in the resonator this cathode supplies a stable emission current of 100 — 200 amp/cm^2. The boride cathode can function in a poor vacuum and at atmospheric pressure when cold. It requires no activation when switched on and the emission is easily monitored by its temperature. The cathode holder 3 was mounted flush with the inner surface of the resonator, precisely in the symmetry plane of the accelerator.

The tantalum strip of the cathode heater was heated by a 427-cycle alternating current with strength up to 50 amp. The magnetic field around the current could perturb electron orbits and deflect electrons from their plane of motion. In order to obviate this defect, the trigger pulse of the modulator was synchronized with the zero phase of the cathode current, at which time the magnetic field vanishes and cannot perturb electron motion, while the cathode temperature and emission remain practically unchanged because of the thermal inertia of the heater. On the other hand, the symmetry of the resonator and cathode adjustments were checked by varying the starting phase and thus perturbing the orbits.

The total cathode emission current and the beam current were recorded oscillographically. The ratio of the current I captured into accelerating orbits to the current I_k emitted from the cathode

$$K = I / I_k$$

is called the capture coefficient, which usually has a value of $1/30$ to $1/40$ in the first mode. Beam losses are usually small during acceleration after the second transit through the resonator. Figure 4 represents the current distribution in different orbits; this was recorded automatically on a target of 5-mm diameter.

The capture coefficient K is determined by two factors, the initial phase region $\Delta\varphi$ within which electrons can be accelerated synchronously and the distribution of cathode emission current during each period of the rf field.

The initial phase region $\Delta\varphi$ was calculated for given parameters of the accelerating field and resonator. In the described modes of operation resonant electrons were emitted at the maximum electric field E in the resonator ($\varphi_0 = 0$ if $E \sim \cos\varphi = \cos\omega t$). The calculated value of $\Delta\varphi$ for the 12th orbit has been given above.

The emitted current distribution during a rf period is determined by processes at the cathode. Since the cathode is not biased, emission evidently occurs only during the positive half-period.

With a field of 380 kv/cm at the cathode in the first mode and 460 kv/cm in the second mode and a current density of ~ 100 amp/cm^2 from the cathode, the current is determined mainly by the cathode temperature and only to a lesser extent by the field strength. The field affects emission through the Schottky effect, which diminishes as the cathode temperature rises.

Emission during the positive rf half-period can be assumed approximately constant. In this case the capture coefficient is practically

$$K \approx \Delta\varphi / \pi.$$

At $\varphi_0 = 0$ nonuniform emission during the half-period only increases the calculated value of K.

We selected $\varphi_0 = 0$ originally in order to simplify the calculations and because we intended to use a cold cathode. In the case of field emission, with exponential current density in strong fields, the entire current from the cathode would be emitted close to the field maximum; thus the phase $\varphi_0 = 0$ would be most advantageous. In the case of a hot cathode, for which emission is only slightly dependent on the field, the calculation shows that an initial phase $\varphi_0 < 0$ should be selected. In this case the region $\Delta\varphi$ can be expanded considerably because of electron bunching in their motion along their initial paths inside of the resonator. The bunching mechanism has been discussed in [16].

Electrons were accelerated at $\varphi \neq 0$ in a flat cylindrical resonator with $R_k = 1.9$ cm and L

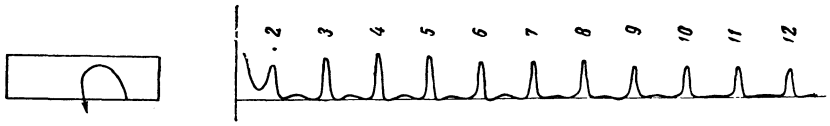

FIG. 4. Current distribution in successive orbits.

= 2.2 cm, with the cathode located farther from the axis than in the case $\varphi_0 = 0$. In this resonator, by varying the magnetic field H from H_0 to 1.5 H_0, the electron energy in the 12th orbit was varied continuously from 6 to 9 Mev with an average current of about 10 ma and capture coefficient $1/30 - 1/20$. Adjustment of the magnetic field was accompanied by a slight shift of the orbits; therefore the orbit ports of the resonator were elongated.

The foregoing modes are of great interest when the beam energy must be varied continuously. With the earlier conventional methods of injection[3] the beam energy was limited to multiples of the rest energy. The more rigorous conditions governing electron capture thus deprived the accelerator of the requisite flexibility.

5. PROPERTIES OF THE ELECTRON BEAM

Electrons in a microtron move within the homogeneous field of the magnet, and the electrons are focused solely by the resonator field, since motion occurs during the zero phases of the electric field.[17]

It should be noted that along the first segment of the trajectory within the resonator (KA in Fig. 2) the vertical motion of electrons is affected by the action of the rf magnetic field; the average effect is a certain amount of beam defocusing along the initial segment. This effect is small, but makes it necessary to position the cathode precisely in the symmetry plane of the resonator and magnet.

The electron orbit ports in the resonator walls are either circular with 10 — 8 mm diameters, or elongated with 18 — 20 mm lengths and 8-mm height. Practically no beam loss resulted from the vertical dimension of the ports. Horizontal focusing was ensured by lengthening of the electron pulses during transits. The beam cross section was 4 × 5 mm in the last orbit. The beam dimensions and orbit positions indicated that the energy spread did not exceed 50 kev in the first mode and 100 kev in the second mode. Some 80% of the beam in the last orbit is easily extracted magnetically through a circular cone (13 in Fig. 1) with soft steel walls. This channel is 500 mm long, with an 8 × 10 mm entrance and 20 × 30 mm exit. The position of the channel in the accelerator is not very critical.

An rf analyzer was used to investigate electron bunching and the charge distribution in bunches accelerated in the first mode.[18] The kinematic design of the accelerator is well confirmed by the measured charge distribution. Most of the charge in a bunch lies within a region 5 — 7 mm long, and the particle density in the bunch is 10^8 cm^{-3}.

The maximum current and energy attainable in a microtron are of interest. Estimates show that because of the strong bunching of the microtron beam, even with currents as low as 1 amp, coherent radiation from bunches moving in a constant magnetic field can be expected to have considerable effect on electron motion.

All bunches progress simultaneously through the resonator, which is thus loaded with a current equal to the beam current multiplied by N, the number of orbits. Interactions between the current and both the resonator and cathode can also limit the range of usefulness of the accelerator, but the extent of this influence requires further study.

6. ACCELERATOR OPERATION AND EFFICIENCY

An accelerator operating mode begins with resonator tuning and excitation of the rated magnetic field. This is followed by adjustment of the cathode current. At a given level of rf power loading the resonator by means of the cathode current, the electric field strength required for resonant acceleration of electrons can be attained. This is accomplished most easily by observing the oscillogram of target and cathode currents or the mean intensity of the beam and of gamma radiation near the target. For low cathode currents the electric field is large and electrons are accelerated only at the beginning and end of each pulse (Fig. 5a). For too high cathode currents, electrons either are not accelerated or are accelerated only at the middle of a pulse (Fig. 5b). With the correct cathode current and electric field in the resonator, acceleration occurs throughout the entire period of stable resonator operation.

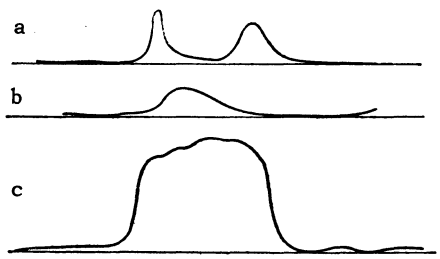

FIG. 5. Shape of current pulses.

Following the adjustment of the cathode current, a further fine adjustment of the resonator in accordance with thermocouple readings usually produces the optimum distribution of power between the load and the resonator. Experience has shown that the established mode is very stable and that the accelerator can function with practically no attention on the part of the operator. Current

pulse duration at the target is usually 1.8 – 2.2 μsec (Fig. 5c).

The field strength in the flat resonator is 300 – 600 kv/cm. In our toroidal resonators the field between the flat or rounded surfaces of the working section of an 8 – 10 mm gap reached 1000 – 1500 kv/cm. No appreciable emission or discharge was detected from the mechanically polished copper surfaces in either case. Cold emission from copper at $E = 10^6$ v/cm is calculated to be $i = 10^{-10}$ amp/cm^2. It is of interest that the field strengths achieved by us in flat resonators are very much higher than the assumed limit[19] of 100 – 150 kv/cm in linear accelerators for field configurations very close to our configuration in each resonator.

Experiments have shown that a lowering of the vacuum to 10^{-4} mm Hg or the absence of a transverse magnetic field was not accompanied by either a discharge or extraneous emission in the flat resonator.

The accelerator efficiency η is determined by the distribution of rf power fed to the resonator. A fraction P_1 of the power is expended in ohmic losses in the resonator walls and, for a given wavelength, depends only on the resonator size and field E. Calculated values of P_1 for the first and second modes are given in Table II for a copper resonator with $\lambda = 10$ cm and depth of penetration $\delta = 1.2 \times 10^{-4}$ cm.

Another fraction P_k of the power is expended in accelerating all emitted electrons in the first segment of their trajectory. We can assume that this fraction equals approximately the product of the emitted current $I_k = I/K$ by the energy $U_1 - U_0$ acquired by the electron in its first passage out of the resonator. The inaccuracy of this estimate lies in the fact that we here neglect the distribution of current and energy with respect to the accelerating-field phase.

The effective power P_a is expended in accelerating resonant electrons, and is the product of three factors, the beam current I, the energy ΔU, and the number N of orbits. The accelerator efficiency is therefore represented approximately by

$$\eta = \frac{P_a}{P_1 + P_k + P_a} = \frac{IN\Delta U}{P_1 + I\Delta U / K + NI\Delta U}.$$

A rise of η will obviously accompany an increase of N, I, or the capture coefficient K. Approximate power distributions and other experimental data are given in Table II.

The current in the 12th orbit of the second mode is considerably lower than the levels attained in the first six orbits. The current loss in the final orbits was evidently associated with defocusing resulting from growing magnetic field inhomogeneity as the field strength became twice as large as the rated value.

The power distribution pertains only to a stable mode. In our case resonator oscillations are built up in a time equal to approximately $1/3$ of the total duration of an rf pulse; this must be taken into account in computing the efficiency of the accelerator. In the cases of pulses that are shorter than this build-up time the accelerator efficiency will decrease; on the other hand, increased pulse duration leads to higher efficiency.

Higher efficiency can result from reduced resonator losses if a toroidal resonator is used with a large shunt resistance across the effective gap. However, the complexity of the field in a resonator of this shape makes it difficult to determine the optimum injection conditions. In a toroidal resonator with a small gap and the conventional geometrical parameters[2,3] it is more advantageous to capture and accelerate electrons from a hot cathode. This is required if we wish to use the condition $\varphi_0 < 0$.

A toroidal resonator with a hot cathode is of interest in the case of an intermittent microtron. In a microtron operating at high levels of pulsed power the reduction of losses in the resonator is not very important.

Microtron modes are also possible in which the magnetic field is stronger than the levels we have indicated. This will be accompanied by higher electron energy without an increase in the number of orbits but, of course, with greater power losses in the resonator.

CONCLUSIONS

The described accelerator is a high-current microtron in which efficient electron acceleration has been achieved for the first time in an operating mode with variable energy increment per cycle. These advantages resulted from the use of an efficient thermionic cathode and exact calculations for motion in a new form of resonator. Experi-

Table II

Mode	N	I, ma	U_{12}, Mev	ΔU, kev	K	U, kev	P_1, kw	P_k, kw	P_a, kw	η, %
1	12	20	7.3	560	1/40	1120	300	465	135	15
2	12	5	13	1000	1/20	500	500	100	65	7

ments performed with this accelerator confirmed the calculations based on an analysis of electron motion in the given electromagnetic field.

The microtron can compete well with linear accelerators at low energies. The principal advantages of the microtron are the constant beam energy, bunching, and the greater operating simplicity and reliability resulting from the simple resonator shape and from energizing by pulsed magnetrons.

In conclusion we wish to thank P. L. Kapitza for supporting this work and S. I. Filimonov for his continued interest. We also wish to thank G. P. Prudkovskii and L. A. Vaĭnshteĭn for useful discussions, A. A. Kolosov and S. V. Melekhin for constant experimental assistance, and engineer L. Zykin for his participation in the construction of the accelerator.

APPENDIX

CALCULATION OF ELECTRON MOTION IN THE MICROTRON

S. P. Kapitza, V. N. Melekhin, I. G. Krutikova, and G. P. Prudkovskii

We shall now present the principal results of the calculations of electron motion in a microtron with a hot cathode. We start with the relativistic equation of electron motion in an electric field **E** and magnetic field **H**:

$$\frac{d}{dt}\frac{m\mathbf{V}}{\sqrt{1-V^2/c^2}} = e\left(\mathbf{E} + \left[\frac{\mathbf{V}}{c}\,\mathbf{H}\right]\right) \qquad (1)^*$$

in which we then introduce the dimensionless variables

$$\varphi = \omega t, \quad x = kX, \quad y = kY, \quad k = \omega/c,$$
$$u = V_x/c, \quad v = V_y/c, \quad \beta^2 = u^2 + v^2,$$
$$\Gamma = U/mc^2 = 1/\sqrt{1-\beta^2}. \qquad (2)$$

We are thus using natural quantities that are characteristic of relativistic electronics.

We also introduce the relative magnetic field strength

$$\Omega = H/H_0, \qquad (3)$$

where $H_0 = \omega mc/e$ is the nominal magnetic field of a microtron at the frequency ω (the cyclotron field). The electric field amplitude divided by the constant magnetic field gives the quantity

$$\varepsilon = E/H. \qquad (4)$$

We investigated electron motion in a circular cylindrical resonator with E_{010} excitation and in a rectangular resonator with E_{101} excitation (see [20], Secs. 93 and 94). In both cases the rf field has only the components E_y and H_z in the XY plane, independently of the Y coordinate. The dimension L of our resonators in the Y direction was very much smaller than the other dimensions; we therefore speak of flat resonators (Fig. 6).

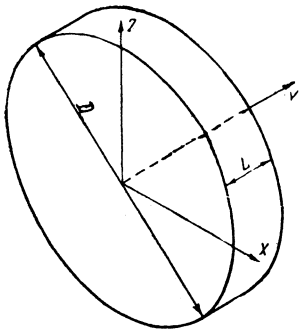

FIG. 6. Cylindrical resonator.

In the cylindrical resonator (1) becomes

$$\frac{d}{d\varphi}\frac{u}{\sqrt{1-\beta^2}} = -\Omega v + \varepsilon\Omega v J_1(x)\sin\varphi,$$
$$\frac{d}{d\varphi}\frac{v}{\sqrt{1-\beta^2}} = \varepsilon\Omega J_0(x)\cos\varphi + \Omega u - \varepsilon\Omega u J_1(x)\sin\varphi. \qquad (5)$$

In the rectangular resonator we have, correspondingly,

$$\frac{d}{d\varphi}\frac{u}{\sqrt{1-\beta^2}} = -\Omega v + \varepsilon\Omega v\varkappa\sin\varkappa x\sin\varphi,$$
$$\frac{d}{d\varphi}\frac{v}{\sqrt{1-\beta^2}} = \varepsilon\Omega\cos\varkappa x\cos\varphi + \Omega u - \varepsilon\Omega u\varkappa\sin\varkappa x\sin\varphi, \qquad (6)$$

with the relative wave number $\kappa = k_x/k_z$.

Equations (5) or (6) describe electron motion completely in the variable field of the resonator and constant magnetic field. The initial conditions depend on the position of the cathode. Neglecting the thermal velocities of the electrons, the initial conditions are $\varphi = \varphi_0$, $x = x_k$, $y = 0$, $u = 0$, and $v = 0$, where x_k is the coordinate of the cathode.

Electron trajectories outside of the resonator are circular up to the point of entrance into the resonator at $y = l = kL$, where L is the resonator thickness.

The cyclic motion is easily programmed for automatic calculation, which was performed with six-place accuracy as far as the 12th orbit. This program permitted the detailed study of the entire acceleration process, since all fundamental factors were taken into account in the equations. The sole simplification that must be mentioned is the neglect of the way in which the rf field is affected by ports in the resonator walls. The field distor-

$^*\left[\frac{\mathbf{V}}{c}\mathbf{H}\right] = \left[\frac{\mathbf{V}}{c}\times\mathbf{H}\right]$.

tions produced by these ports are small and do not affect the results essentially. We also did not take into account the interaction between electrons and radiation emitted by electrons while we were considering the motion of a charge in a given field.

Electron motion is entirely dependent on five parameters—the fields Ω and ϵ, the resonator dimension l, the cathode position x_k, and the initial phase φ_0. In the microtron accelerating mode (sometimes called a mode with variable energy increment[7]) these parameters are independent. Moreover, motion along the first segment of the trajectory within the resonator can be considered separately, being calculated in such a way that upon leaving the resonator the electron enters into the accelerating mode.

We shall write the relations between the accelerator parameters (field strengths, transit phase, and resonator dimensions) characterizing this mode. In each transit the energy of an electron possessing the stable phase φ_s is enhanced in such a way that the period of revolution in a field H is increased by q periods ($T = 2\pi/\omega$) of the variable field. We confine ourselves to the fundamental mode $q = 1$,[9] where the phase-stable region is largest and the energy increment for each transit is

$$\Delta U = eHcT/2\pi \quad \text{or} \quad \Delta\Gamma = \Omega. \tag{7}$$

We shall also determine the energy increment when a fast electron moves along the axis $x = 0$ through a resonator of length l. Integrating the second equation in (5) from the entrance phase φ_n to the exit phase φ_m for $v \approx -1$, while neglecting terms that would take into account the effect of the magnetic field, we obtain

$$\Delta\Gamma \approx \varepsilon\Omega\,(\sin\varphi_n - \sin\varphi_m).$$

In view of (7), after transforming the expression in parentheses, we obtain

$$\sin(l/2) = 1/2\varepsilon\cos\bar{\varphi}, \tag{8}$$

where $\bar{\varphi} = (\varphi_m + \varphi_n)/2$ and $\varphi_m - \varphi_n \approx l$.

The mean phase $\bar{\varphi}$ is determined by the requirement of phase stability during subsequent acceleration, and in the absence of phase oscillations φ should be equal to the stable phase φ_s. On the basis of our calculations and from the theory of phase oscillations in a microtron[7,8] we can take

$$\varphi_s = 0{,}35\,(20°), \qquad \cos\varphi_s = 0.94, \tag{9}$$

Equation (8) enables us to relate l and ϵ immediately. It is also evident that the resonator thickness l has no bearing on the initial segment of the trajectory if the electron does not strike the wall.

Electron energy at the end of the first transit can be called the injection energy (pertaining to the given system): its dimensionless value should be

$$\Gamma_1 = 2\Omega \text{ (first type of trajectory)},$$
$$\Gamma_1 = \Omega \text{ (second type of trajectory)}. \tag{10}$$

These conditions are associated with the fact that an electron must encircle the resonator in its first revolution.

For phase stability of the motion the exit phase φ_{ex} for the first type and the entrance phase φ_1 for the second type of trajectory must satisfy approximately the conditions

$$\varphi_{ex} \approx \varphi_s + l/2 \text{ (first type)},$$
$$\varphi_1 \approx \varphi_s - l/2 \text{ (second type)}. \tag{11}$$

Conditions (7) — (11) together with the solution of (5) or (6) provide a basis for deriving the parameters Ω, ϵ, l, x_k and φ_0, corresponding to what we shall call the resonant trajectories of the microtron accelerating mode. It is not necessary to calculate all orbits and the parameter l can be omitted from consideration.

We have calculated only the trajectories with $\varphi_0 = 0$, corresponding to electron exit at the maximum electric field amplitude in the resonator. Table III gives the results for two modes of the first type and one mode of the second type in the circular resonator, and for one mode of the second type in the rectangular resonator.

The resonant trajectory regions for the first mode with $\varphi_0 = 0$ are shown in Fig. 7 in the coordinates Ω and x_k. The resonant region $\Gamma = 2\Omega$ is determined by the following three conditions: Electrons must depart with initial phases within the stable acceleration region ($0.25 < \bar{\varphi} < 0.45$), the exit point must be close to the axis ($-0.2 < x_{ex} < 0.3$), and the extreme point of the orbit within the resonator must lie within the wall ($y_{max} < l$). The corresponding region of values of Ω and x_k is shaded in the figure; the heavy dots represent the experimental operating modes for which data are given in the table.

Figure 8 shows the small resonant trajectory region for the second mode in the cylindrical resonator with $\varphi_0 = 0$, corresponding to the large value $\Omega = 1.9$. The dot represents an experimental result consistent with the calculation.

Figure 9 shows a similar region for the rectangular resonator with $a = 0.9\lambda$ and $b = 0.6\lambda$, in which Ω has still larger values (2.02). This was not confirmed experimentally.

Table III

Type of motion	Type of resonator	Ω	ε	x_k	l	$\Delta\varphi$	z_{ex}	w_{ex}
1	cylindrical	1.10	1.11	1.20	1.00	0.07	0.183	0.031
1	cylindrical	1.10	1.06	1.10	1.05	0.07	0.178	0.029
2	cylindrical	1.81	0.80	0.20	1.45	0.24	—	—
2	rectangular	2.02	0.79	0.20	1.47	0.21	—	—

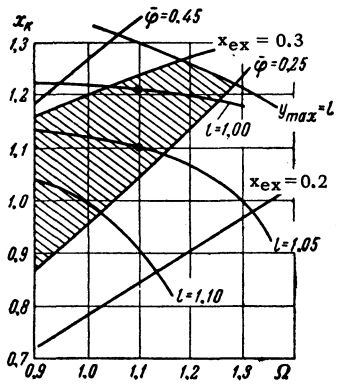

FIG. 7. Region of resonant trajectories for the first type of motion (with $\varphi_0 = 0$) in a cylindrical resonator.

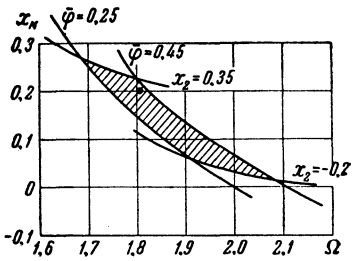

FIG. 8. Region of resonant trajectories for the second mode (with $\varphi_0 = 0$) in a cylindrical resonator.

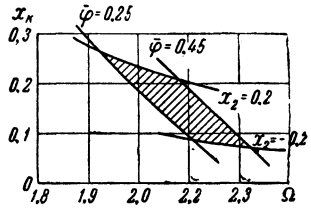

FIG. 9. Region of resonant trajectories for the second mode (with $\varphi_0 = 0$) in a rectangular resonator.

The foregoing modes can be investigated in detail by means of complete exact calculations for several orbits, in order to check the correctness of the preliminary parameters determined from relations some of which, specifically (8) and (11), are only approximate.

Phase oscillations for the first mode are shown in Fig. 10 for $\varphi_0 \sim 0$. By varying φ_0 and finding the boundary of the stable trajectory region we determine the region of electron capture given in the table for N = 12.

In Fig. 10 the phase stable region is outlined with a dashed curve. If the phase trajectory of an electron crosses this limiting line or lies outside of it the electron will sooner or later depart from synchronism and will be lost. The initial points of the phase trajectories lie along straight lines intersecting the limiting curve at two points where the values of φ_0 determine the region of capture. The exact locations of the straight lines depend on x_k, the cathode position, as shown in Fig. 10.

Stable trajectories cannot be determined by numerical computations for an unlimited number of orbits. In practice, however, we are always interested in electron behavior and acceleration during a finite number of revolutions. For example, Fig. 10 shows that the trajectory for $\varphi_0 = -0.04$ and $x_k = 1.10$ begins to depart from synchronism only after twelve revolutions. The tra-

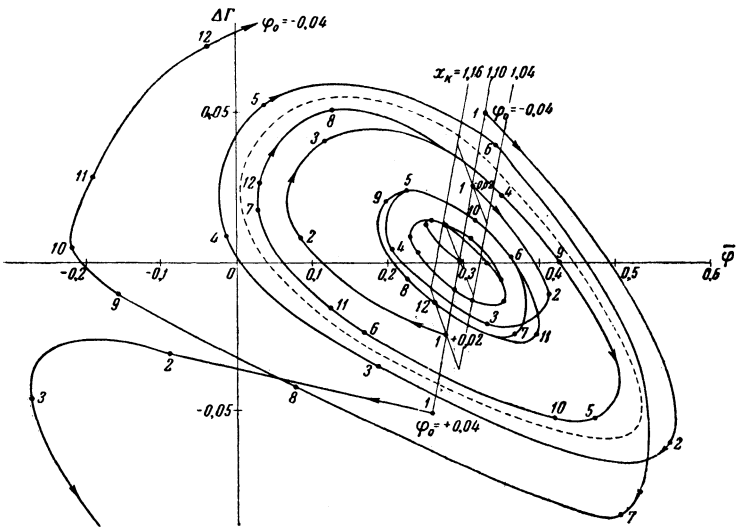

FIG. 10. Phase oscillations of electrons in the first accelerating mode.

jectory will therefore be useful up to this number of orbits, although it is unstable from a formal point of view. The existence of such "limited" trajectory stability accounts for the small current drop always observed between successive orbits. One can therefore speak more properly not of a stability region, but of the dynamic aperture of the accelerator, i.e., the region of initial parameters corresponding to electrons accelerated during a given number of orbits.

Figure 11 shows the position of orbits around the resonator for different numbers N. The orbits are seen to lie very close to the resonator axis.

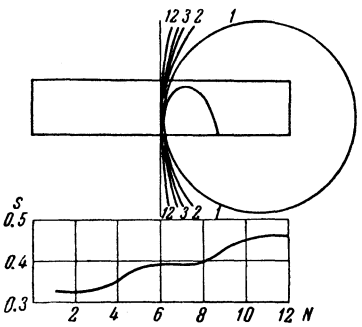

FIG. 11. Positions of orbits and drift of orbit centers.

It is interesting to consider the drift of the center of circular orbits along the y axis in a rf field. Figure 11 shows the position of the center s (the value of which is highly exaggerated along the y axis) as a function of N for a stable trajectory. The slow regular shift of the center is accompanied by oscillations with the period $\Delta N \sim 5$, which are evidently associated with the phase oscillations of the electron.

A constant uniform field does not affect the vertical motion of electrons in a microtron. An rf electric field, unlike that in linear accelerators, performs a focusing function because $\varphi_S > 0$. During acceleration an electron traverses the focusing field of the entrance port at a higher value of the field strength than the defocusing field at the resonator exit. According to Bell's calculations [17] electrons oscillate slowly near the median xy plane with amplitudes that grow slowly as $\Gamma^{1/4}$.

During motion in the first segment of the trajectory, the variable magnetic field H_θ in a circular resonator and H_x in a rectangular resonator perturb motion in the vertical direction whenever the particle departs from the xy plane.

The linearized equations of vertical motion in a circular resonator are, with $z = kZ$,

$$\frac{d}{d\varphi}\frac{w}{\sqrt{1-\beta^2}} + Az = 0, \quad w = \frac{dz}{d\varphi}, \quad A = -\varepsilon\Omega\frac{J_1(x)}{x}v\sin\varphi. \tag{12}$$

The variation of the coefficient $A(\varphi)$ along the trajectory is shown in Fig. 12. Focusing by the acting forces occurs along a part of the trajectory ($A > 0$), while defocusing occurs elsewhere ($A < 0$). The corresponding solution of (12) can be obtained by numerical integration along the first segment of the trajectory. Table III gives values of z_{ex} and w_{ex} derived for the initial conditions $z_0 = 0.1$ and $w_0 = 0$.

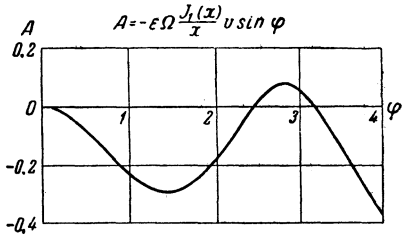

FIG. 12. Variation of the coefficient determining the vertical motion of an electron in the initial segment of its trajectory for the first type of motion in a cylindrical resonator.

The overall effect of the variable magnetic field on the first segment of the trajectory is a slight defocusing; this has been calculated only approximately, since defocusing produced by space charge, which we have neglected, is also possible close to the cathode. The vertical defocusing limits the cathode size and determines the height of the orbit ports of the resonator. Experiment indicates adequate focusing by rf fields during acceleration under actual conditions.

It is also of interest to calculate the power required to excite a suitable rf field. The power loss can be determined by integrating the magnetic field H_θ on the resonator surface (see Sec. 98 of [20], for example):

$$P = \frac{c^2}{32\pi^2}\frac{1}{\sigma d}\oint |H_z|^2 ds, \tag{13}$$

where σ is the conductivity of the metal and $d = (1/2\pi)\sqrt{\lambda c/\sigma}$ is the depth of penetration.

Using the expression for fields in a cylindrical resonator and integrating, we obtain

$$P = \frac{\pi}{4}\nu_{01}J_1^2(\nu_{01})\frac{d}{\lambda}(\nu_{01} + l)\,\Omega^2\varepsilon^2 P_0, \tag{14}$$

where ν_{01} is the first root of the zeroth order Bessel function, and $P_0 = m^2c^5/e^2 = I_0V_0 = 8700$ Mw is the characteristic power of rf electronic devices. This power is independent of the wavelength λ and equals the energy flux transported through a cross section $8\pi\lambda^2$ of a flat wave, whose field is $mc^2/e\lambda$. The power can be represented as the product of the characteristic electron current $I_0 = mc^3/e = 17\,000$ amp by the voltage ($V_0 = 511$ kev) corresponding to the electron rest energy.

Since l depends only on ϵ according to Eq. (8), the power depends only on ϵ and Ω. For an accelerator with a cylindrical resonator operating in a mode of any type we obtain the power

$$P = 1.02\, P_0 \frac{d}{\lambda}\left(1.2 + \arcsin \frac{1}{1.88\,\varepsilon}\right)\varepsilon^2\Omega^2. \qquad (15)$$

The dependence of the ratio $P\lambda/P_0 d$ on Ω and ϵ is shown in Fig. 13.

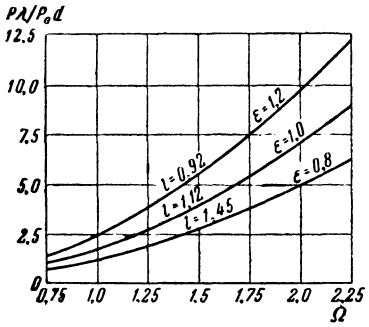

FIG. 13. Ohmic power loss in a cylindrical resonator vs the parameters Ω and ε of an electron accelerating mode.

For copper at room temperature we have $\sigma = 5.7 \times 10^5\,\Omega^{-1}$ cm. Also, for $\lambda = 10$ cm we have $d = 1.2 \times 10^{-4}$ cm and $P_0 d/\lambda \approx 100$ kw. An expression analogous to (15) can also be derived for a rectangular resonator:

$$P = \frac{\pi^2}{8} P_0 \frac{d}{\lambda}\left[\frac{a^2+b^2}{2ab} + \frac{l\,(a^3+b^3)}{a^2b^2}\right]\varepsilon^2\Omega^2, \qquad (16)$$

where a, l, and b are the lengths of the resonator along the x, y, and z axes, respectively. The shape of the resonator has only a small effect on the power, which is influenced most strongly by the parameter Ω. For large Ω, with the previous number of orbits, the energy is increased by the factor Ω compared with the nominal value at $\Omega = 1$. It should be noted that $\epsilon \sim 1$ is always valid; therefore the power loss depends mainly on Ω, the relative magnetic field strength.

Our calculations provided a basis for proposing a microtron resonator differing considerably from all previously suggested and constructed resonators. For this resonator the rf field amplitude ϵ and the associated accelerating gap l in their dimensionless form are close to unity. The length of the transit distance $L = l/k$ therefore considerably exceeds the values proposed and realized by other authors.[7,21] For a given wavelength the accelerating field is correspondingly weaker; the relative reduction is a very favorable factor in enlarging the useful range of an accelerator that can be achieved with higher fields and frequencies.

The value of ϵ is close to unity because a microtron is a cyclic accelerator in which the electric field is not small. This is the fundamental difference between microtrons and other cyclic accelerators of relativistic particles, and makes it difficult to analyze microtrons by the approximation methods that commonly consider an adiabatic accelerating process in accelerators with weak fields. We therefore developed computer procedures for numerical calculations.

On the other hand, the numerical approach required resonators with simple geometrical shapes, in which the expressions for the field ϵ are known. In these resonators a given accelerating voltage requires somewhat higher rf power than in specially selected toroidal resonators. However, the possibility of a complete calculation in this case produces a considerable gain in the final accelerating parameters. We can thus exceed the empirical limits of all previously proposed microtrons, whose currents and efficiencies were found to be more than one order of magnitude smaller than those based on the foregoing calculations.

We can expect that the further development of numerical methods for resonators of all shapes will lead to an accelerating unit that is optimal with respect to rf power dissipation. All calculating difficulties can be overcome.

In conclusion we wish to express our gratitude to P. L. Kapitza and E. S. Kuznetsov for their interest, to M. M. Antimonik for the programming of calculations, and to V. P. Bykov and L. A. Vaĭnshteĭn for useful discussions.

[1] V. I. Veksler, DAN SSSR **43**, 346 (1944); J. Phys. (U.S.S.R.) **9**, 153 (1945).

[2] Redhead, Le Caine, and Henderson, Can. J. Research **A28**, 73 (1950).

[3] Henderson, Heymann, and Jennings, Proc. Phys. Soc. (London) **B66**, 654 (1953).

[4] H. F. Kaiser, Rev. Sci. Instr. **25**, 565 (1955).

[5] D. Aitken and R. E. Jennings, Nature **181**, 1726 (1958).

[6] A. Carrelli and F. Porreca, Nuovo cimento **6**, 729 (1957).

[7] Henderson, Heymann, and Jennings, Proc. Phys. Soc. (London) **B66**, 41 (1953).

[8] A. A. Kolomenskii, J. Tech. Phys. (U.S.S.R.) **30**, 1347 (1960), Soviet Phys.-Tech. Phys. **5**, 1278 (1961).

[9] Kotov, Kuznetsov, and Rubin, Usp. Fiz. Nauk **64**, 197 (1958).

[10] Kapitza, Bykov, and Melekhin, JETP **39**, 997 (1960), Soviet Phys. JETP **12**, 693 (1961).

[11] D. K. Aitken, Proc. Phys. Soc. (London) **A70**, 550 (1957).

[12] A. Poulin, Nuclear Instr. and Methods **5**, 107 (1959).

[13] V. P. Bykov and V. N. Kostryukov, Pribory i Tekhnika Éksperimenta (Instr. and Exptl. Techniques) **3**, 154 (1959).

[14] G. P. Prudkovskii, Collection, Nekotorye Voprosy Inzhenernoĭ Fiziki (Some Problems of Engineering Physics), Moscow Physics and Engineering Institute, No. 2, 1957, p. 36.

[15] H. Reich, Z. angew. Phys. **11**, 481 (1960).

[16] S. P. Kapitza, J. Tech. Phys. (U.S.S.R.) **29**, 729 (1959), Soviet Phys.-Tech. Phys. **4**, 654 (1959).

[17] J. S. Bell, Proc. Phys. Soc. (London) **B66**, 802 (1953).

[18] V. P. Bykov, JETP **40**, 1658 (1961), Soviet Phys. JETP **13**, 1169 (1961).

[19] Chodorow, Ginzton, Hanse, Kyhl, Neal, and Panofsky, Rev. Sci. Instr. **26**, 134 (1955).

[20] L. A. Vaĭnshteĭn, Elektromagnitnye Volny (Electromagnetic Waves), Soviet Radio, Moscow, 1957.

[21] A. Poulin, Nuclear Instr. and Methods **9**, 113 (1960).

Translated by I. Emin
72